Giant and supergiant lattices on graphite

J. Xhie, K. Sattler, M. Ge, and N. Venkateswaran
Department of Physics and Astronomy, University of Hawaii at Manoa, Honolulu, Hawaii 96822
(Received 7 December 1992)

Anomalous giant lattices have been observed on four separate samples of highly oriented pyrolytic graphite with scanning tunneling microscopy. They exhibit hexagonal symmetry with lattice constants of 1.7, 2.8, 3.8, and 6.6 nm. Atomic resolution of graphite was obtained simultaneously. Kuwabara, Clarke, and Smith [Appl. Phys. Lett. **56**, 2396 (1990)] have suggested that those superperiodic features may be Moire patterns due to rotational misorientation of the top layer relative to the underlying graphite single crystal. In this paper we present (1) evidence for the misorientation of the graphite top layer which causes the observed giant lattices, (2) a complete description to account for detailed features of these giant lattices, (3) observation of a supergiant lattice superimposed on the atomic and giant lattices, and (4) adsorption of cobalt particles on the giant lattice.

I. INTRODUCTION

The (0001) surface of highly oriented pyrolytic graphite (HOPG) has been imaged extensively using the scanning tunneling microscope (STM). STM images of graphite often reveal unusual features such as large atomic corrugation[1,2] asymmetry in the apparent heights of neighboring carbon sites,[3] and superstructures near defects.[4] More recently, anomalous large-scale periodic patterns have been observed on graphite in addition to its atomic structure.[5-10] They had hexagonal symmetry with periodicities up to 44 nm and occurred in regions with observable boundaries. Kuwabara, Clarke, and Smith[5] suggested that the observed superperiodicities may be rotational Moire patterns resulting from the overlap between a misoriented top layer of graphite and the underlying graphite single crystal. Since the STM can only image the top layer, the relative rotation of this layer to the underlying graphite cannot be directly shown in the STM images. Therefore, the suggestion of Moire patterns remained a speculation.

In this paper we report similar superperiodic patterns, which we call "giant lattices," obtained from four separate graphite samples. We show first evidence of a misorientation of graphite that results in the observed giant lattice. We also show that, although the STM can only image the top layer, the effects from deeper layers on a misoriented top layer can lead to giant lattices in the STM images. A complete description is developed to explain the detailed features of giant lattices observed with STM. In addition to the atomic and giant lattices, a third periodic pattern—"supergiant lattice"—was also observed on one of the samples.

The anomalous giant lattices may provide a unique system for adsorption of clusters because their lattice constants are comparable to the size of clusters. On one of our samples, cobalt was deposited on the surface and cobalt clusters were imaged together with the giant lattice. This enables us to determine the adsorption sites of clusters on such a giant lattice.

II. EXPERIMENT

The four graphite samples which we used were prepared independently. The first sample was cleaved in a high-vacuum (2×10^{-8} torr) chamber. A small amount of cobalt was evaporated onto the surface leading to the formation of cobalt particles. These particles were of size 1–5 nm and were randomly distributed on the surface. Then the sample was transferred to a STM,[11] mounted in an ultrahigh vacuum (5×10^{-10} torr) chamber, without breaking the vacuum. The images were obtained in ultrahigh vacuum at room temperature using a Pt-Ir tip. The tunneling current was kept at 4.5 nA and the bias voltage was varied from -500 to 200 mV.

The second sample was cleaved in air and then transferred to a STM (Ref. 12) operating at ambient conditions. The images were obtained with a silicon tip at a positive tip bias voltage of 2.5 V and a tunneling current of 4.6 nA.

The third sample was prepared in a high-vacuum (2×10^{-7} torr) chamber by vapor deposition of cobalt on a freshly cleaved graphite substrate, similar to that for the first sample. After deposition it was analyzed by x-ray photoelectron spectroscopy (XPS), which showed a coverage of less than 5% of a cobalt monolayer on the graphite surface. The STM images were taken in air at room temperature with a Pt-Ir tip at a positive tip bias voltage of 54 mV and a tunneling current of 1.8 nA.

The fourth sample was also prepared in a similar way as for the first sample except that instead of cobalt, a small amount of carbon was deposited onto the surface. The STM images were taken in ultrahigh vacuum at room temperature with a Pt-Ir tip. The bias voltage and tunneling current were maintained around 120 mV and 2 nA, respectively.

For all four samples, the STM's were operated at constant-height mode where the tip was maintained at a constant separation from the surface, and the variation of the tunneling current was recorded. The STM images presented in this paper were all taken from the first sample except that Fig. 4 was taken from the fourth sample.

0163-1829/93/47(23)/15835(7)/$06.00

III. RESULTS AND DISCUSSION

A. Giant lattice

Figure 1 shows a large-scale STM image taken from the first sample. A sharp boundary which appears as a straight array of highlighted bright spots divides the image into two parts. The region on the right-hand side of the boundary exhibits a hexagonal giant lattice constant of 3.8 nm. On the left-hand side of the boundary, images at atomic scale were taken. They showed a regular graphite atomic structure. The giant lattice extended over an area of at least 500×500 nm^2 and was very stable. The variation in the bias voltage from -500 to 200 mV did not cause any significant change in the images.

A closer view of the giant lattice in Fig. 1 is displayed in Fig. 2(a). In a unit cell shown as the hexagon in the picture, there are three different sites which appear similar to the sites in the atomic image of graphite. The white spots at three corners of the hexagon resemble the β sites in the atomic lattice and the gray areas at the other three corners resemble the α sites. The dark area at the center of the hexagon resembles the hole site. This can be seen in Fig. 2(b) where a section is taken along the line *AB* indicated in Fig. 2(a). We use g-h-site, g-α-site, and g-β-site as notations for the "hole site," "α site," and "β site" in the giant lattice, respectively, to distinguish them from those in the atomic lattice. The giant corrugation is 1.2–1.4 nm and the atomic corrugation is 0.2–0.3 nm, both with respect to their hole sites.

An even closer view, with atomic resolution, is shown in Fig. 3. The angle between the giant and atomic lattices is $\sim 28°$. The atomic rows in the lattice appear twisted, especially along the direction that has the smallest angle to the scan line (horizontally from left to right). This twisting can be reduced significantly by changing the scan parameters such as increasing the scan rate and scan size or decreasing the feedback gains. Therefore, the enhanced twisting along that direction is most likely a scan effect due to the high corrugation amplitude of the giant lattice.

The giant lattices observed on the other samples were also of hexagonal symmetry but with different lattice constants of 6.6, 1.7, and 2.8 nm. They were rotated about 27°–28° relative to the atomic lattice and extended over a region of up to a few hundred nm. The corrugation was typically 4–5 times stronger compared to the atomic corrugation. The sharp boundaries which were observed in all cases suggest that grain boundaries or steps on the graphite surface may have existed, separating giant from regular lattices.

The suggestion of rotational Moire patterns,[5] in principle, is a reasonable approach because (1) it provides a good explanation for the observed various superperiodici-

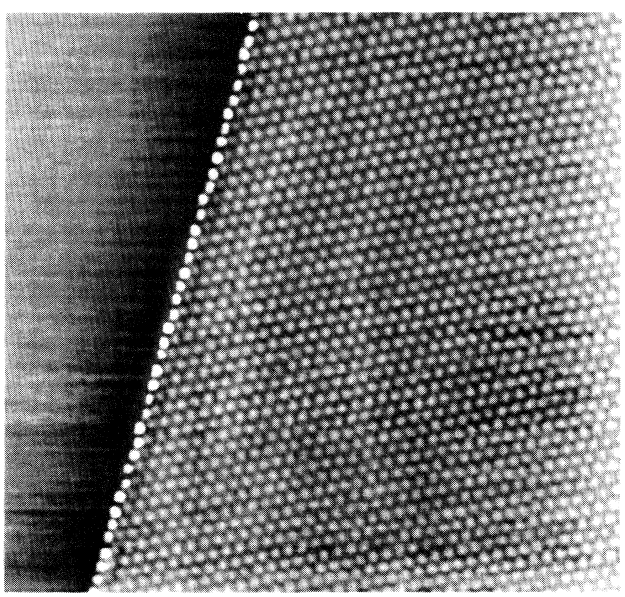

FIG. 1. A STM image (160×160 nm^2) showing a sharp boundary that separates the giant lattice from regular graphite. The giant lattice on the right-hand side of the boundary exhibits a hexagonal symmetry with a lattice constant of 3.8 nm.

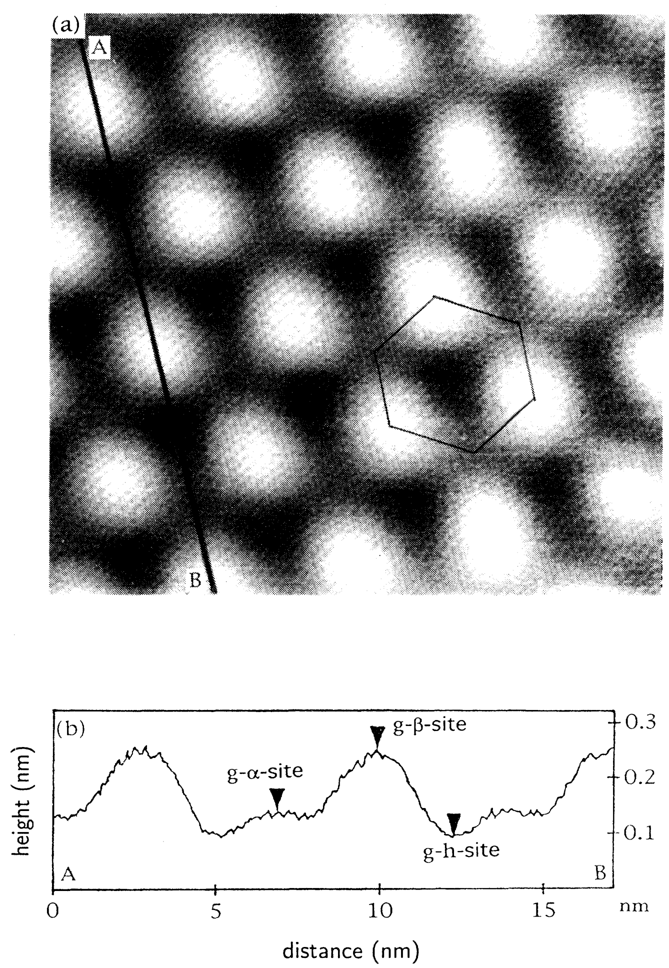

FIG. 2. (a) A closer view (17×17 nm^2) of the giant lattice in Fig. 1. The hexagon shows a unit cell of the giant lattice. (b) A height plot along the line *AB* indicated in (a).

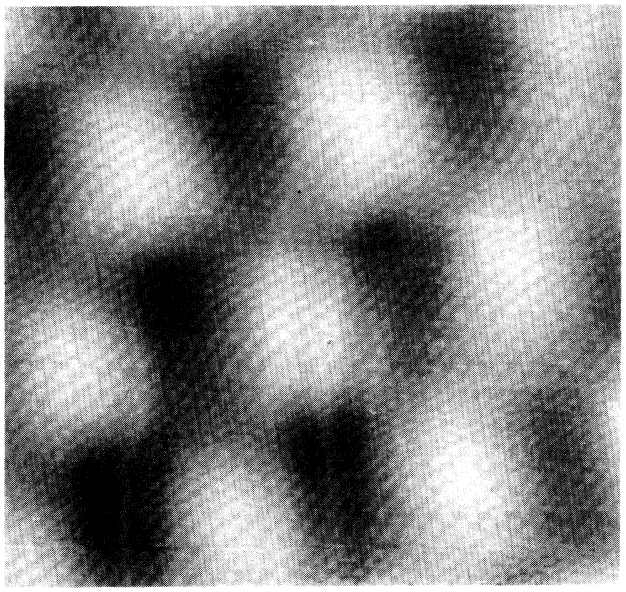

FIG. 3. A STM image (10×10 nm^2) showing both the giant and atomic lattices.

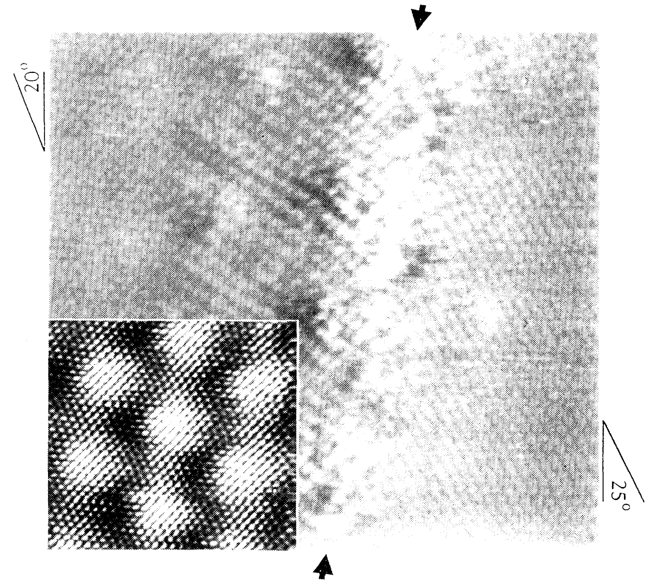

FIG. 4. A STM image (11×11 nm^2) taken near a boundary of a giant lattice (left-hand side) with a lattice constant of 2.8 nm. The inset shows an overview (7×7 nm^2) of this giant lattice taken at the left-hand side of the boundary. The atomic lattices on both sides of the boundary are clearly seen and are misoriented relative to each other by $\sim 5°$. The superstructures near the boundary are due to periodic charge-density modulations associated with the boundary.

ties, and (2) the weak coupling between graphite layers could facilitate such small misorientations of the top layer. However, direct observation of a rotated top layer relative to underlying graphite has not been obtained in any of the STM studies of giant lattices. This is because electron tunneling with the STM occurs only between the tip and the first layer of graphite, and the atoms in deeper layers cannot be observed.

Near a boundary, however, it is possible for the STM to image atomic lattices of graphite on both sides of the boundary simultaneously. The orientation of the two lattices can be compared to find out whether there exists a misorientation, and if so, whether the misorientational angle is related to the observed giant lattice. Fig. 4 shows such an image taken from the fourth sample. The boundary is shown as indicated by the arrows on the top and bottom of the image. The region on the right-hand side of the boundary shows the regular graphite lattice. On the left-hand side of the boundary, a giant lattice with a lattice constant of 2.8 nm was observed as shown in the inset. In order to image the atomic lattices, we increased the bias voltage significantly. As a result, the giant lattice on the left-hand side of the boundary is not clear in this image. Also, it is not clear if the boundary is associated with an atomic step or a grain boundary because superstructures of graphite are dominant in this region and extend to a few nm next to the boundary. Such superstructures are frequently found on graphite near steps, grain boundaries, or any defects on the surface. They are attributed to periodic charge-density modulations induced by defects on the graphite surface.[4] Besides the superstructures, the atomic lattices on both sides of the boundary are clearly seen and their orientation can be compared. As indicated by the angles on both sides of the image, the atomic lattices are misoriented by $\sim 5°$. For two lattices of spacing d misoriented by an angle θ, the period D of the produced Moire pattern is given by an expression $D = d/[2\sin(\theta/2)]$.[5] Substituting $d = 0.245$ nm and $\theta = 5°$ into the above equation, we get $D \approx 2.8$ nm. This value is in good agreement with the measured lattice constant, 2.8 nm, of the giant lattice. Therefore, we conclude that the observed giant lattice is a result of misorientation of the graphite top layer.

On the other hand, since the STM sees only the top layer and is unable to reveal a pattern which is formed by two overlaid lattices,[13] the giant lattices observed with STM do not directly correspond to Moire patterns. In the following text we show that although the atoms in deeper layers are not imaged, they may influence the apparent structure of the surface in the STM images. We concentrate on three structural aspects to account for such influences.

1. *Symmetry of the giant lattices*

Graphite is a layered material and carbon atoms in each layer form a honeycomb structure. The single crystal of graphite is formed by a $ABAB \cdots$ stacking of these layers, where every other layer is laterally shifted by one nearest-neighbor distance. Figure 5(a) shows a schematic drawing of the surface of graphite. The structure of the surface is composed of two hexagonal lattices: an α sublattice consisting of atoms with neighbors directly below in the next layer; and a β sublattice consisting of atoms without such neighbors. A side view cut along the direction indicated by the arrow is shown in the inset.

If the top layer is slightly rotated, the regular $ABAB\cdots$ stacking of graphite layers becomes $CABAB\cdots$, where C is used as notation for the rotated top layer. A Moire pattern can be produced by overlapping the C layer onto the next A layer. Since the distinction between α and β sites is due to the $ABAB\cdots$ stacking, the C layer is considered to be a honeycomb lattice without such a distinction. The resulting Moire pattern with the C layer rotated $\sim 3.5°$ is shown in Fig. 5(b). It displays a giant honeycomb structure, as indicated by the

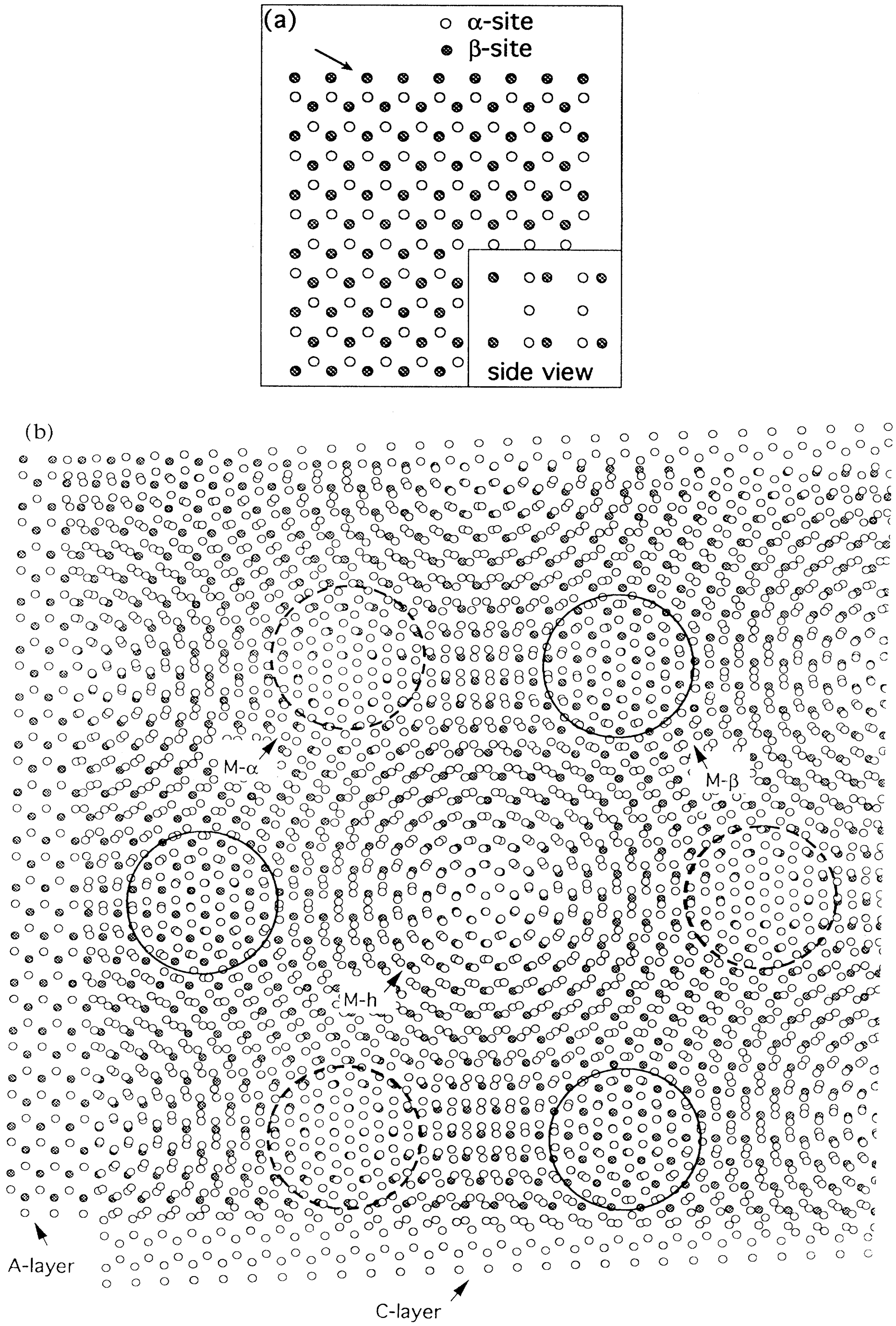

FIG. 5. (a) A schematic drawing of the surface structure of graphite. A side view is shown in the inset. (b) A Moire pattern produced by overlapping two lattices. One of them (C layer) has a honeycomb structure and the other (A layer) has the structure shown in (a). The two lattices are rotated relative to each other by 3.5°.

six large circles. The regions in the large solid circles are different from those in the large dashed circles. In the large solid circles, each α atom in the A layer is covered or partially covered by an atom in the C layer. In the large dashed circles, each β atom in the A layer is covered or partially covered by an atom in the C layer. Similar to the atomic structure of the graphite surface, the large honeycomb structure of the Moire pattern is composed of two hexagonal lattices: a sublattice represented by the large dashed circles; and another sublattice represented by the large solid circles. The giant honeycomb forms a unit cell of the Moire pattern. We call the centers of the large dashed circles "M-α-sites," the centers of the large solid circles "M-β-sites," and the center of the giant honeycomb "M-h-site." Therefore, the Moire pattern in Fig. 5(b) displays a hexagonal symmetry with three different sites in a unit cell. Such a symmetry comes from the distinction between α and β sites of the second layer and is consistent with the symmetry of the observed giant lattices in STM images as, for example, in Fig. 2(a).

2. *Atomic sublattice in the presence of the giant lattice*

Although α and β atoms are geometrically identical at a regular graphite surface, β atoms appear at a higher intensity than α atoms in STM images. The asymmetry in the apparent intensity of the α and β atoms is due to their distinction resulting from the $ABAB\cdots$ stacking of graphite layers. Each α atom in the top layer sits directly above an α site in the second layer, while each β atom sits above a hole site. This leads to the difference in their electronic states. The β atoms have a higher density of states in the energy range scanned by the STM and therefore appear brighter in STM images.[3]

In the case where the top layer is rotated, the situation becomes much more complicated. As is shown in Fig. 5(b), an atom in the top layer can find itself above any site in the second layer. For example, it can be above a hole site, an α site, a β site, or anywhere in between these sites. For an atom above a hole site, it would show maximum intensity in the STM images just like β atoms in a regular graphite lattice. Similarly an atom above an α site would show less intensity and an atom above a β site would show the least intensity.

With such an order of intensity in mind, we are now able to look closely at the M-h-sites, M-α sites, and M-β sites in the Moire pattern. In a region at the M-h site, atoms of the top layer are either above α sites of the next layer or above β sites. Those above the α sites give higher intensity in the STM images and form a hexagonal lattice. In a region at the M-α site (M-β site), atoms of the top layer are either above hole sites of the next layer or above β sites (α sites). The atoms above the hole sites give higher intensity in the STM images and also form a hexagonal lattice. Therefore a hexagonal atomic lattice is expected throughout all three regions in the Moire pattern. This is in good agreement with the observed atomic structure in actual STM images. In Fig. 3, for example, a hexagonal atomic lattice is seen all over the image despite the presence of the giant lattice.

In addition to the atomic lattice, the regions at M-β sites of the Moire pattern should give a higher average intensity than any other regions. They correspond to g-β sites of a giant lattice in STM images as, for example, Fig. 2(a). Similarly the regions at M-α sites give the second-highest intensity on average and the regions at M-h sites give the minimum average intensity. They correspond to g-α sites and g-h sites of a giant lattice in STM images, respectively.

3. *Orientation of the giant lattice relative to the atomic lattice*

The relative orientation of giant with respect to atomic lattice provides additional information as to whether a misoriented top layer would be the cause of the giant lattice. If so, their relative orientation should be consistent with that predicted by the rotational Moire patterns. For a giant lattice with lattice constant in the range of 1.7–6.6 nm, the corresponding misorientational angle θ should be 3°–6°. The orientation of the giant lattice relative to the atomic lattice is then $30°-\theta/2$, i.e., 27°–28.5°. This is in good agreement with our observation.

From the discussion on the three structural aspects, we have shown that all the features of giant lattices observed with STM can be explained by small misorientations of the top layer relative to the underlying graphite. The causes of the misorientation of graphite, however, are not known and may come from various processes such as cleavage or some peculiarity in the growing process of graphite. In addition, the superperiodicity introduced by a misoriented top layer may also induce an electronic redistribution, which leads to the very high corrugation of the giant lattice compared to the atomic corrugation.

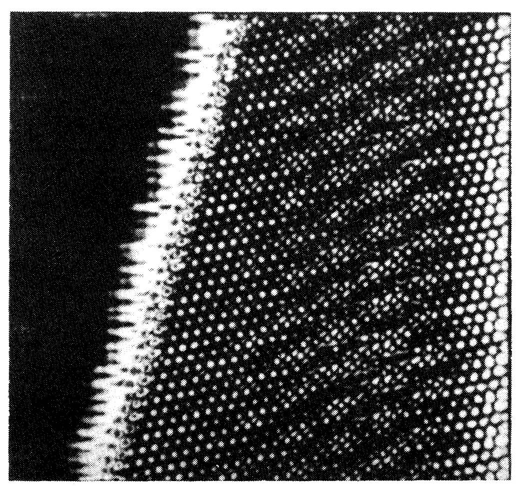

FIG. 6. A contour STM image (160×160 nm^2) similar to Fig. 1. The region at the right-hand side of the boundary shows a supergiant lattice superimposed on the giant lattice. The corrugation of the super pattern is extremely small, $\sim1/10$ of the corrugation of the giant lattice. In order to bring out the effect, a high-contrast (narrow black and white intensity lines) contour scale is used, which also leads to the bright bands at the boundary and at the right-hand side of the image.

B. Supergiant lattice

In addition to the giant and atomic lattices, a supergiant lattice was also observed on the first sample. Figure 6 is a contour STM image showing such a supergiant lattice. It appears on the right-hand side of a boundary similar to that of Fig. 1 and is superimposed on the giant lattice. It exhibits a distorted hexagonal pattern with a periodicity of ~ 15 nm. The corrugation amplitude is ~ 0.1 nm, much less than the corrugation amplitude of the giant lattice. The supergiant pattern appeared in a number of images and scaled with various scan sizes. It was found only in the region where the giant lattice was observed, for example, only on the right-hand side of the boundary in Fig. 5. The physical mechanism of such a supergiant lattice is not quite understood. It could be a result of the strain produced by the small rotation of the top layer.[14]

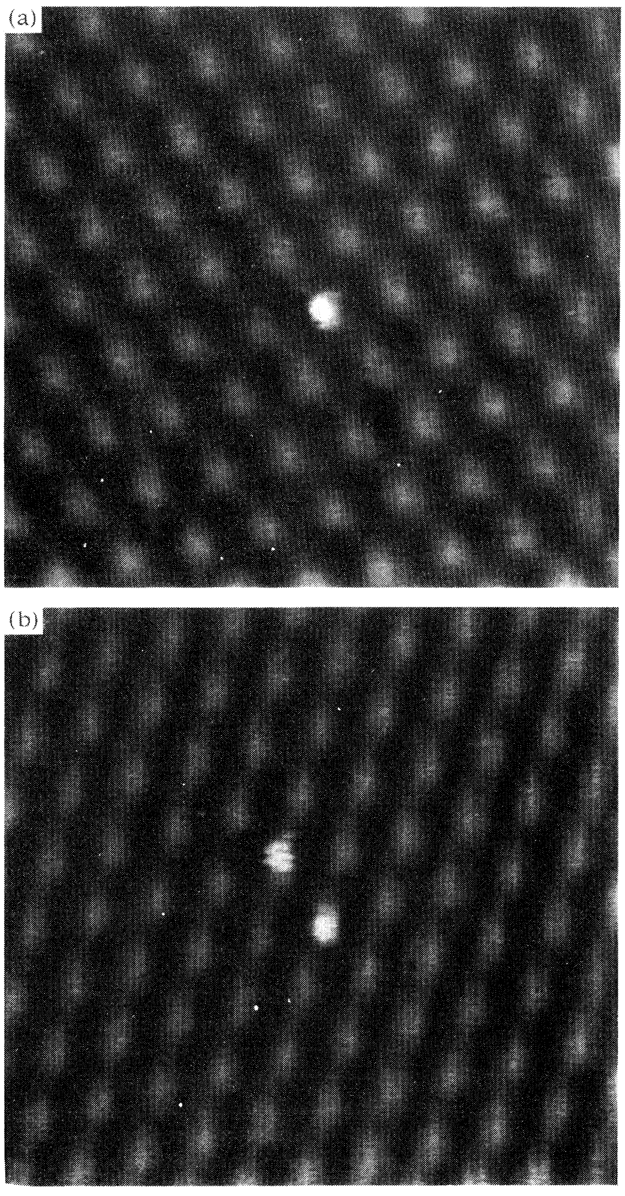

FIG. 7. (a) A STM image (33×33 nm^2) showing a single cobalt particle on the giant lattice. (b) A STM image (33×33 nm^2) showing two cobalt particles on the giant lattice.

C. Adsorption sites of cobalt particles

Since cobalt was also deposited on the first sample, small cobalt particles were found occasionally on the surface together with the giant lattice. Figure 7(a) shows an image of a single cobalt particle of size $1-1.5$ nm. It appears as the bright spot at the center of the image. Figure 7(b) is an image of two cobalt particles of similar size. In both images the cobalt particles were found on the top sites (g-β sites) of the giant lattice. This is very similar to the observation of single atoms and atomic dimers of noble metals on the surface of graphite. They were mostly found at the top sites (β sites) of the graphite atomic lattice.[15,16] Single atoms and atomic dimers prefer β sites in the atomic lattice because the β sites have a higher local density of states at the Fermi level than the other sites. For cobalt particles, their much larger size makes it impossible to bond to any atomic site. But the presence of the giant lattice provides a similar environment to that of the atomic lattice to single atoms and dimers. For the same reason, the cobalt particles locate themselves on g-β sites. This suggests that high local density of states at the Fermi level may determine the adsorption sites for both atoms and clusters.

IV. CONCLUSION

Giant lattices have been observed on four graphite samples with scanning tunneling microscopy. They showed hexagonal symmetry with lattice constants of 1.7, 2.8, 3.8, and 6.6 nm. These giant lattices are due to small misorientations of the top layer relative to the underlying graphite single crystal, and a complete description is developed to account for their detailed features. In addition, a supergiant lattice superimposed on the giant and atomic lattices has also been observed. It showed a stretched hexagonal pattern with a periodicity of ~ 15 nm. Cobalt particles on the surface were found on the top sites of the giant lattice, suggesting that high local density of states at the Fermi level may determine the adsorption sites.

ACKNOWLEDGMENTS

Financial support from the Office of Technology Transfer and Economic Development (OTTED) of the University of Hawaii, from the Research Council of the University of Hawaii, and from the U.S. National Science Foundation, Grant No. DMR-9106374, is gratefully acknowledged.

[1]J. M. Soler, A. M. Baro, and N. Garcia, Phys. Rev. Lett. **57**, 444 (1986).

[2]J. Tersoff, Phys. Rev. Lett. **57**, 440 (1986).

[3]D. Tomanek, S. G. Louie, H. J. Mamin, D. W. Abraham, R. E. Thomson, E. Ganz, and J. Clarke, Phys. Rev. B **35**, 7790 (1987).

[4]J. Xhie, K. Sattler, U. Muller, N. Venkateswaran, and G. Raina, Phys. Rev. B **43**, 8917 (1991).

[5]M. Kuwabara, D. R. Clarke, and D. A. Smith, Appl. Phys. Lett. **56**, 2396 (1990).

[6]J. W. Lyding, J. S. Hubacek, G. Gammie, S. Skala, and R. Brockenbrough, J. Vac. Sci. Technol. A **6**, 363 (1988).

[7]T. Hashizume, I. Kamiya, Y. Hasegawa, N. Sano, T. Sakurai, and H. W. Pickering, J. Microsc. **152**, 347 (1988).

[8]V. Elings and F. Wudl, J. Vac. Sci. Technol. A **6**, 412 (1988).

[9]J. E. Buckley, J. L. Wragg, and H. W. White, J. Vac. Sci. Technol. B **9**, 1079 (1991).

[10]P. I. Oden, T. Thundat, L. A. Nagahara, S. M. Lindsay, G. B. Adams, and O. F. Sankey, Surf. Sci. Lett. **254**, L454 (1991).

[11]McAllister Technical Services, Coeur d'Alene, Idaho.

[12]Digital Instruments, Inc., Santa Barbara, California.

[13]When a double tip was scanning over different grains in the vicinity of a grain boundary, the STM images showed Moire patterns. Such Moire patterns contributed to simultaneous imaging of the double tip; T. R. Albrecht, H. A. Mizes, J. Nogami, S.-I. Park, and C. F. Quate, Appl. Phys. Lett. **52**, 362 (1988).

[14]O. L. Alerhand, D. Vanderbilt, R. D. Meade, and J. D. Joannopoulos, Phys. Rev. Lett. **61**, 1973 (1988).

[15]E. Ganz, K. Sattler, and J. Clarke, Phys. Rev. Lett. **60**, 1856 (1988).

[16]U. Muller, K. Sattler, J. Xhie, N. Venkateswaran, and G. Raina, J. Vac. Sci. Technol. B **9**, 829 (1991).

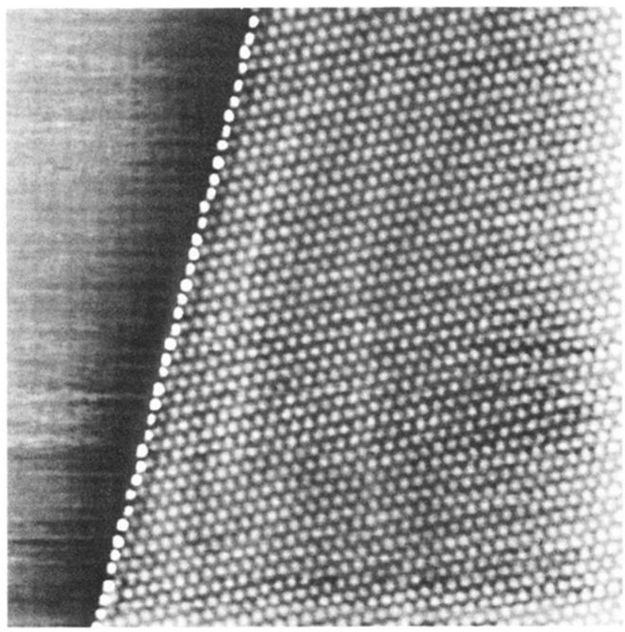

FIG. 1. A STM image (160×160 nm^2) showing a sharp boundary that separates the giant lattice from regular graphite. The giant lattice on the right-hand side of the boundary exhibits a hexagonal symmetry with a lattice constant of 3.8 nm.

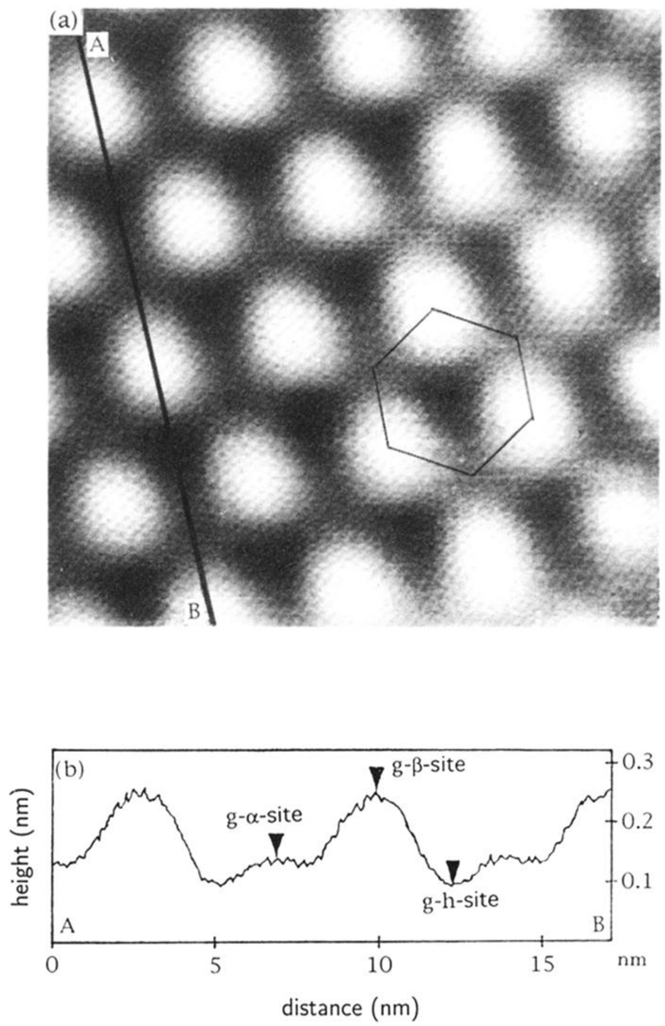

FIG. 2. (a) A closer view (17×17 nm^2) of the giant lattice in Fig. 1. The hexagon shows a unit cell of the giant lattice. (b) A height plot along the line AB indicated in (a).

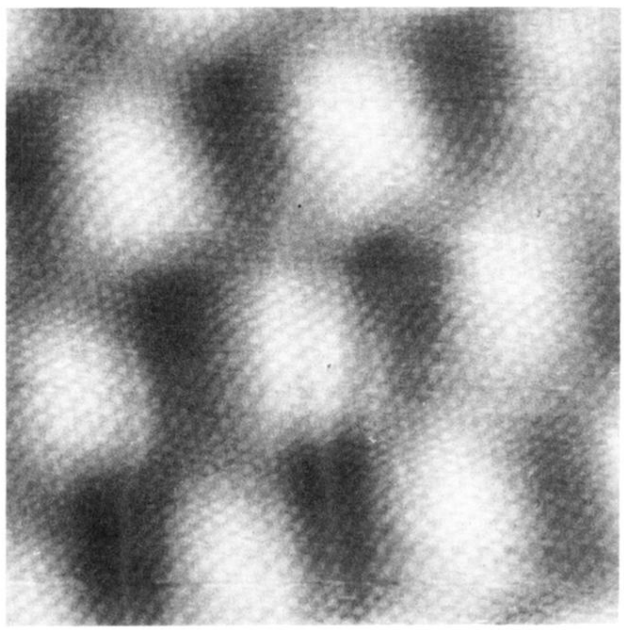

FIG. 3. A STM image (10×10 nm^2) showing both the giant and atomic lattices.

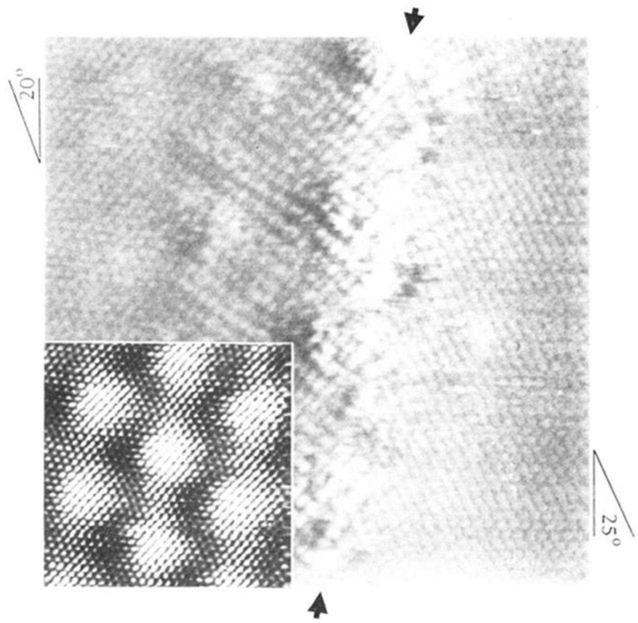

FIG. 4. A STM image (11×11 nm^2) taken near a boundary of a giant lattice (left-hand side) with a lattice constant of 2.8 nm. The inset shows an overview (7×7 nm^2) of this giant lattice taken at the left-hand side of the boundary. The atomic lattices on both sides of the boundary are clearly seen and are misoriented relative to each other by $\sim 5°$. The superstructures near the boundary are due to periodic charge-density modulations associated with the boundary.

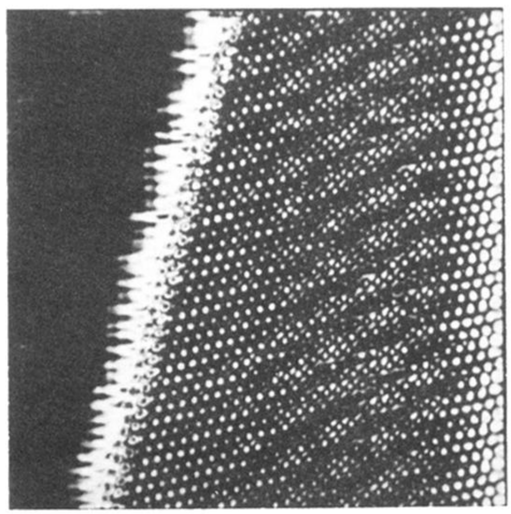

FIG. 6. A contour STM image (160×160 nm^2) similar to Fig. 1. The region at the right-hand side of the boundary shows a supergiant lattice superimposed on the giant lattice. The corrugation of the super pattern is extremely small, $\sim 1/10$ of the corrugation of the giant lattice. In order to bring out the effect, a high-contrast (narrow black and white intensity lines) contour scale is used, which also leads to the bright bands at the boundary and at the right-hand side of the image.

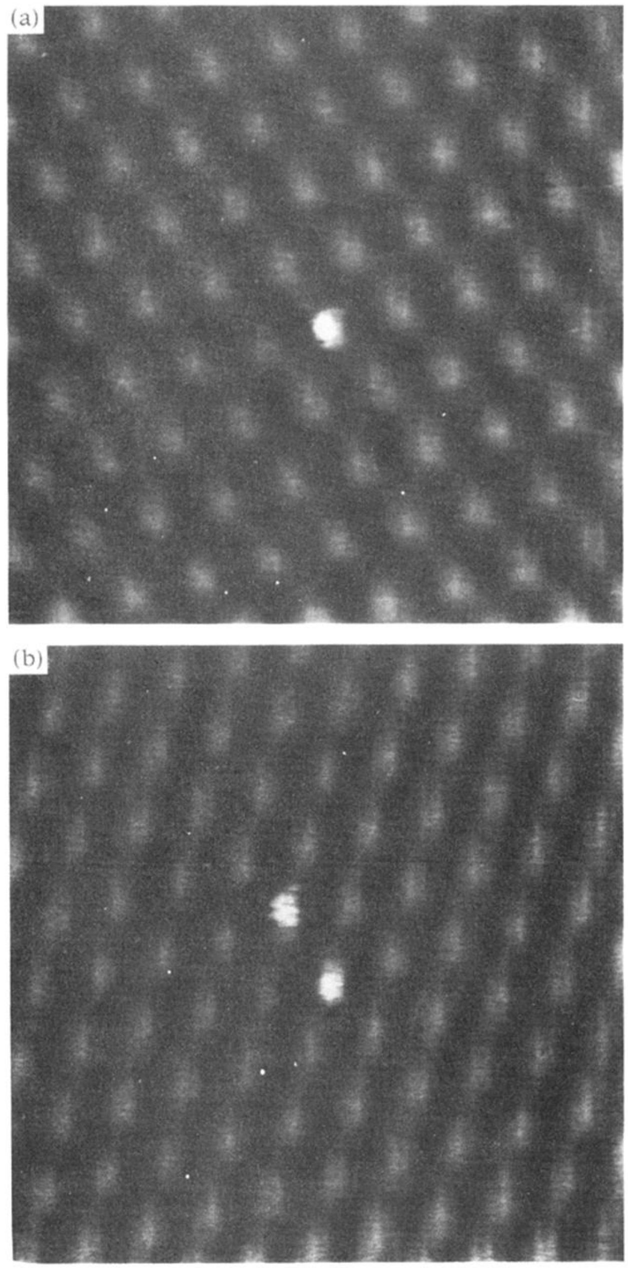

FIG. 7. (a) A STM image (33×33 nm^2) showing a single cobalt particle on the giant lattice. (b) A STM image (33×33 nm^2) showing two cobalt particles on the giant lattice.